Journal of Fluorescence, Vol. 11, No. 1, 2001

Temperature and Base Sequence Dependence of 2-Aminopurine Fluorescence Bands in Single- and Double-Stranded Oligodeoxynucleotides

Mikako Kawai,[1] Michael J. Lee,[1] Kervin O. Evans,[1] and Thomas M. Nordlund[1,2]

Received February 4, 2000; revised August 21, 2000; accepted August 21, 2000

Fluorescence excitation spectra of 2-aminopurine (2AP) incorporated into single-stranded DNA di- and trinucleotides, as well as into single- and double-stranded pentanucleotides, have been measured as a function of temperature from 5 to 65 °C. Spectral shifts have been precisely quantitated through difference spectroscopy and spectral fits. G(2AP)C and C(2AP)G oligonucleotides have relatively blue-shifted excitation spectra (especially the former) compared to the 2AP free base. The position of the excitation peak of 2AP free base is temperature independent, those of (2AP)T, G(2AP)C, C(2AP)G and TT(2AP)TT shift about 0.4 nm to the blue from 5 to 65 °C, though the spectra of the G-C-containing oligomers also change shape. The temperature dependence of the A(2AP)T spectral position is 2.5-times stronger, and just rises to that of the free base at high temperature. On the other hand, the decrease of yield with increasing temperature is smallest for A(2AP)T, even compared to the free base. The dominant effect when A neighbors 2AP appears to be temperature-dependent stacking with accompanying energy transfer, while in G- and C-containing trinucleotides a temperature-independent interaction keeps the 2AP excitation spectrum blue-shifted. The effect of double strand formation appears to be small compared to stacking interactions. These spectra can be useful in identifying base neighbors and structures of 2AP in unknown 2AP-labeled DNA.

KEY WORDS: Spectroscopy; spectral shifts; DNA; nucleic acids; base stacking; adenine.

INTRODUCTION

Fluorescence probes have been used for a variety of purposes in proteins, from simple location and quantitation of the protein, to determination of degree of binding and conformational change, to precise measurement of distances and distance distributions. Probes have been of two sorts, intrinsic (usually tryptophan and tyrosine) and extrinsic (derivatives of dyes such as fluorescein, rhodamine, etc.). Naturally-occurring tryptophan and tyrosine have the advantage of not perturbing the structure they are intended to monitor. Intrinsic probes have been used to provide signals tracking degree of binding or extent of conformational change through spectroscopic changes (intensity or peak wavelength). Quantitative determination of atomic-resolution structure in proteins through fluorescence spectroscopy (peak positions) has not generally been possible, however, because (i) tryptophan and tyrosine spectra are broad and complex, and (ii) the structural possibilities in proteins are almost limitless. Naturally-occurring and inserted tryptophans have been used to determine interatomic distances, but this has been as an energy-transfer donor to additional extrinsic probes [1–9]. In those last applications, fluorescence provided detailed structural information which could only be

[1] Department of Physics, University of Alabama at Birmingham, Birmingham, Alabama 35294-1170.
[2] To whom correspondence should be addressed. Fax: 205-934-8042. E-mail: nordlund@uab.edu

1053-0509/01/0300-0023$19.50/0

obtained with great difficulty from multi-dimensional NMR or X-ray crystallography, the leading Angstrom-resolution molecular structural methods. The dominant modern application of fluorescence probes in DNA has been sequencing—the identification of base types and DNA fragment sizes [10–14]. This identification is made possible, at its core, by understanding the enzymology of DNA replication, however, not by understanding the fluorescence spectroscopy of the DNA probes.

Fluorescence of 2-aminopurine inserted at specific DNA sites which interact with enzymes has been used in a number of elegant experiments to demonstrate the time course and mechanism of protein-DNA interaction. By placing 2AP at various distances from the binding site of T7 RNA polymerase, Ujvari and Martin [15] and Jia et al. [16] demonstrated limited DNA helix melting in a section of the promoter near the transcription start site. Binding constants and kinetic-rates of the polymerase were also obtained. These experiments relied mostly on fluorescence intensity measurements. Allan et al. used fluorescence anisotropy to measure temporal couplings between DNA binding and base flipping with the EcoRI DNA methyltransferase [17]. Other collaborations used fluorescence anisotropy and intensity changes to characterize details of complex protein-nucleic acid interactions, including helicase activity, the proofreading pathway catalyzed by EcoRI DNA methyltransferase, bacteriophage T4 DNA polymerase, and DNA polymerase I (Klenow fragment) [18–25]. 2-Aminopurine has also been used as a probe because of its mutagenic activity [26–30], so it is clear that this useful fluorescence probe should be used carefully.

Fluorescence spectroscopy—the measurement of spectral positions and intensities—is in principle more useful in DNA than in protein structural studies because the conformational possibilities in DNA are few in comparison to proteins. Even when simple, gross fluorescence intensity or anisotropy changes are measured, as in the experiments just described, it is the details of the spectroscopy that provides the explanation of the interactions and structural changes. Spectroscopy provided the basis for the claim that intensity increases upon protein-DNA binding reflected helix melting. Spectroscopy provides the explanation for apparently anomalous results when 2AP is inserted next to guanine [15,31] (and this work). Careful observation of fluorescence spectra also reveals completely new signatures, such as energy and electron transfer bands, which can be used to probe DNA UV damage mechanisms and radical migration, electronic materials properties of DNA and sunscreen activity [31–34]. This work presents straightforward, though precise, fluorescence spectroscopic measurements which can reveal certain aspects of the local structure in single-stranded DNA near the fluorescence probe 2-aminopurine. The information includes identification of the neighboring bases and degree of stacking of A. We emphasize *straightforward* methodologies that can be used in virtually any laboratory equipped with a good-quality fluorometer. Although machine stability must be closely watched, precision data analysis can be done on Excel spreadsheets or virtually any modern, commercial graphing program. We will shortly present additional information on the conformation of oligonucleotides and, by extension, longer strands of DNA, that is revealed in more sophisticated experiments, time-resolved fluorescence and 2D proton NMR. Previous work with pure DNA oligomers has shown how to distinguish double- from single-stranded DNA,[3] 2AP exposure to water, and local mobility, [15,25,35–42].

Two general types of fluorescence changes occur when the temperature of a 2AP-containing sample is varied: the intensity, and the shape and wavelength of the excitation and emission bands. The fluorescence excitation spectrum has proved to be more sensitive to structural changes than the emission spectrum, changing up to about 15 nm (300 to 315 nm) [31,32,39,40] as temperature, stacking and/or solvent are changed. Hydrogen bonding of the (ground-state) 2AP base with water and interaction with a neighboring guanine seem to be the major causes of the bluer excitation spectra, while strong base stacking favors redder spectra and lower fluorescence yield [39,43–45].

The intent of the present study is to demonstrate simple, and generally useful, fluorescence spectroscopic methods which differentiate between 2AP incorporated next to different normal DNA bases in ss DNA and between 2AP in ss and ds DNA. Small spectral shifts are shown to be quite easily quantifiable using software available virtually everywhere (Excel). In short, ss oligonucleotides, the temperature dependence of the difference fluorescence excitation spectrum distinguish between various bases neighboring the 2-aminopurine. Furthermore, the ss oligonucleotides have a weaker temperature dependence of the peak position than a short, ds oligonucleotide. Such results can be useful to demonstrate, for example, that the DNA near a 2AP site is locally unwound, or to distinguish fluorescence emission between two 2APs incorporated at different sites on a piece of DNA. The results will be of practical use to

[3] Distinguishing the two major effects of DNA unwinding, reduction of base stacking and of base pairing, has not always been clearly done. It appears to these authors that the major spectroscopic effects of DNA unwinding on 2AP fluorescence stem from base-stacking changes.

the biochemist/biophysicist studying DNA structure and interactions at the molecular level, though they may not be entirely satisfying to the spectroscopy purist wishing to understand the mechanisms for the spectral perturbations.

MATERIALS AND METHODS

2-Aminopurine free base was used as purchased from Sigma Chemical Co., while 2AP-containing oligodeoxynucleotides for the present work were obtained from Macromolecular Resources (Colorado State University, Ft. Collins, CO). The latter were provided purified by reverse-phase liquid chromatography and characterized by MALDI mass spectrometry. Our own NMR measurements of these oligomers (unpublished) show very low levels of impurities, allowing collection of high-quality proton 2D NMR spectra. Samples were dissolved in 20 mM pH 7.4 Tris-Cl buffer containing 100 mM KCl and 0.1 mM EDTA. Single-stranded concentrations were approximately 10 μM for fluorescence measurements. Single strand concentrations can be found from the 260-nm extinction coefficients of Puglisi and Tinoco [46], with extinction coefficients of 2AP-containing strands from Xu and Nordlund [47]. The concentration of a 2AP-containing strand can also be quickly approximated from the 305-nm absorbance of 2AP, using $\varepsilon_{305} \approx 7.2 \times 10^3$ M^{-1} cm^{-1}. For the duplex pentamer TT(2AP)TT/AATAA, a 1.6-fold excess of the non-fluorescent complementary strand was added to encourage pairing of the 2AP-containing strand. The resulting higher absorbance at 260 nm results in a moderate fluorescence inner-filter effect in the 250–270-nm region. As we are not concerned with the spectrum in this region, we have not corrected the spectra for the duplex.

Absorption spectra and melting determinations were measured with a Response II spectrophotometer (Gilford/Corning, Walpole, MA) with built-in, computer-controlled thermoelectric temperature controller, using 1.0-nm bandwidth and 1.0-cm path length cuvets. Spectra were transferred to a PC and imported into an Excel spreadsheet for further analysis and plotting. Fluorescence spectra were measured with a Fluoromax 2 fluorometer (SPEX/ISA, Inc., Edison, NJ), in either 0.2 × 1.0-cm or 0.3 × 0.3-cm cuvets, typically using 3.0-nm excitation and emission bandwidths and recording in 2-nm steps. Temperature was controlled by a Neslab RTE-5DD circulator (Newington, NH). Sample vs. bath temperature calibration was done by placing a thermistor probe (Omega, Stamford, CT) in a water-filled cuvet and measuring both temperatures.

Data Analysis

Since spectral changes of 2AP-DNA are potentially small, we employ two readily-available means for precise quantitation. The first is a difference method, where each spectrum, recorded as a function of temperature, is subtracted from a reference spectrum, usually the average of several spectra taken near a high or low temperature limit. As has been shown many times, if an approximately Gaussian-shaped spectrum shifts by an amount which is small compared to its width, the amplitude of the difference spectrum is proportional to the shift [40,48]. In the presence of amplitude changes, the spectra must be normalized to find the spectral shift. Since the shift found by this method is relative to the presently unknown peak of the reference spectrum, the spectral change found by this method is fundamentally relative, not absolute. Once the peak or centroid of the reference spectrum is obtained, the relative shifts can be converted to absolute shifts. Spectral bands of organic molecules like 2AP can only expected to be Gaussian when plotted as a function of photon energy or wavenumber. Furthermore, shifts caused by interactions of the chromophore with its environment are fundamentally shifts in energy, so spectra acquired by a fluorescence spectrometer as a function of wavelength should, in principle, be converted to a function of energy or wavenumber. The wavenumber $\tilde{\nu}$ is defined by $\tilde{\nu} = (1/\lambda)$, with λ wavelength in cm. The intensity in wavenumber space $\tilde{I}(\tilde{\nu})$ is obtained from the intensity in wavelength space $I(\lambda)$ using $\tilde{I}(\tilde{\nu}) = (1/\lambda^2)I(\lambda) = \nu^2 I(1/\tilde{\nu})$ and is normalized.

In the present application of the difference method, an average of the spectra at 5°, 10°, and 15° Celsius is normalized and used as a reference spectrum. Calibration of the difference amplitude in terms of wavenumber shift is done by artificially shifting the reference spectra several times and subtracting the original reference spectrum from each artificially-shifted spectrum. Using this data the slope is calculated from a graph of $\Delta\bar{\nu}$ = slope*ΔI vs. ΔI, where $\Delta\bar{\nu}$ is the shift of wavenumber and ΔI is the difference spectral amplitude, taken as the average amplitude over a small interval near the peak. The actual wavenumber shifts of the real spectra, taken as a function of temperature, are then found from multiplying this slope by the difference amplitude found for the (really) shifted spectra. For presentation purposes, we re-convert to plots as a function of wavelength. If spectral changes are small, substantially the same results can be obtained by directly processing spectra as a function of wavelength, using $\Delta\lambda = \beta^*\Delta I$, where β is the slope of the wavelength shift vs difference spectral amplitude. For the oligomers studied here, the value of β, which reflects the shape of the

spectrum, spanned a narrow range of 27.2 to 30.3 nm per unit difference spectral amplitude. The value of β found previously for the deoxy $[CTGA(2AP)TTGAG]_2$ oligomer was 28.1 [49].

The second method for finding spectal shifts involves a simple fit of, e.g., a Gaussian or inverted parabolic function to each spectrum as a function of wavenumber over the top 10% of the spectral amplitude. The Gaussian is, in principle, a superior descriptor of spectra, but if the objective is merely to find the peak, the parabolic fit near the peak is adequate. We use this in the present analysis, since the parabolic fit, but not the Gaussian, is found in virtually all spreadsheet and graphing programs.

The advantages of the difference method lie in its precision and sensitivity, in intermediate steps, to spectral shape changes and/or multiple, overlapping bands, in addition to spectral shifts. The shape changes are clearly visible in the difference spectra as departures from antisymmetry with respect to the zero crossing point of the difference. In the end, the difference method also ignores the spectral shape changes, but at least one knows of the potential problem. If the original recorded spectra are symmetric, the difference method accurately finds the shift of the spectra in terms of the peak and centroid, which are the same. If the original spectra are asymmetric, or if a spectral shape change occurs, the shift is of a quantity somewhere between the peak and centroid. Figure 1 shows artificial difference spectra resulting from two different types of spectral changes. In Fig. 1a, a gaussian centered at 32787 cm^{-1} (305 nm) was shifted by ± 200 cm^{-1} and the resulting spectra subtracted from the unshifted. To obtain Fig. 1b, a spectrum constructed from the original 32787 cm^{-1} gaussian plus a 10% admixture of a second gaussian centered at 31746 cm^{-1} (315 nm) was altered by changing the fraction of the minor gaussian to 5% and 15%. This clearly produces asymmetric difference spectra in these artificial spectra. These asymmetric shifts reflect the changing spectral shape, and resultant shift of the centroid of the spectrum. As shown in later figures, the presence of nearby bands from other excited states in real, 2AP-containing oligomers usually prevents determination of whether our experimental spec-

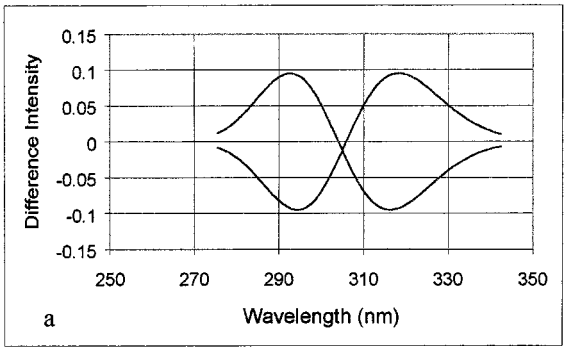

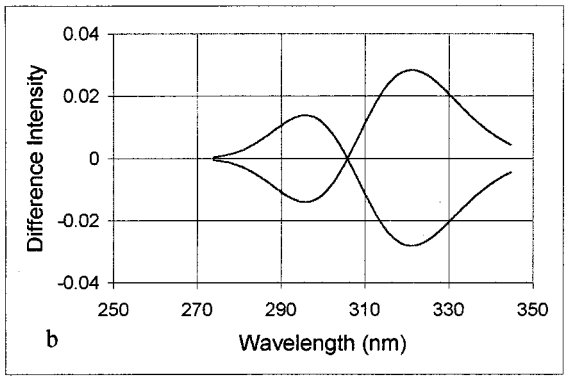

Fig. 1. (a) Difference spectra for ideal, shifted gaussian spectra. The original gaussian is centered (in wavenumber space) at 32,787 cm^{-1}, corresponding to 305 nm, halfwidth 1800 cm^{-1}. The spectrum was then subtracted from gaussians shifted by ± 200 cm^{-1} to created the difference spectrum shown, replotted vs. wavelength. (b) Difference spectra from 32,787 cm^{-1} gaussian with a 5% and 15% admixture of an additional gaussian centered at 31,746 cm^{-1}. Spectra constructed by subtracting a 10%-admixed spectrum from the 5% and 15% admixed. All spectra normalized to peak height of 1.00.

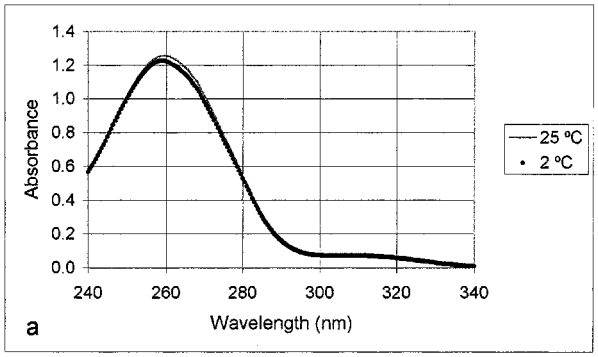

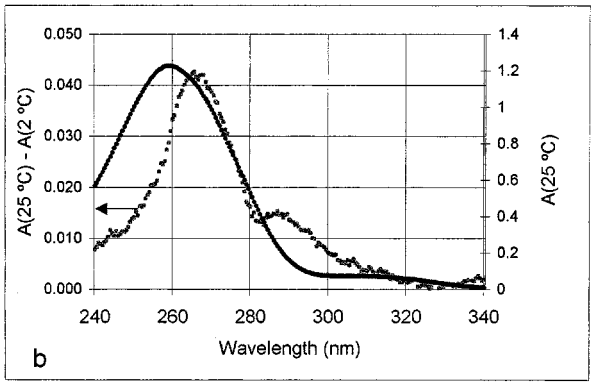

Fig. 2. (a) Absorption spectra of TT(2AP)TT/AATAA duplex pentamer at 2° (upper curve) and 25°C. (b) The 25°C spectrum and difference of absorption spectra at 2° and 25°C. The difference spectrum has peaks at about 266 and 287 nm.

tra shift or change shape (or both). In applications such as the present, such details can often be ignored, as the goals of the investigation are to differentiate between sets of similarly-shaped spectra which change quite differently with temperature, not to determine exact centroids and peaks. The difference method naturally finds amplitude changes, which are also needed. A fundamental limitation of the difference method is the need to obtain a high signal-to-noise ratio reference spectrum, which ideally reflects some pure state. If temperature-dependent spectra reach a high (or low) temperature limit, then the average of spectra near this limit provide a good, high S/N ratio reference. If this is not the case, repeated measurement of a spectrum at one temperature and averaging of the results suffices.[4] The advantage of the peak-fitting method is simplicity and familiarity. The precision of the parabolic fit can rival that of the difference method. However, its chief weaknesses are its complete ignorance of spectral shape changes and its dependence on the number of data points (fraction of the spectrum) fit. Unless shape changes in the originally-recorded spectra are obvious to the eye, one is oblivious to potential complications. As will be seen with the data, the two methods do not produce identical temperature dependencies, primarily due to the peak-shift *vs* shape-change sensitivity discussed above. Nevertheless, both methods clearly distinguish the spectral changes in the oligonucleotides studied.

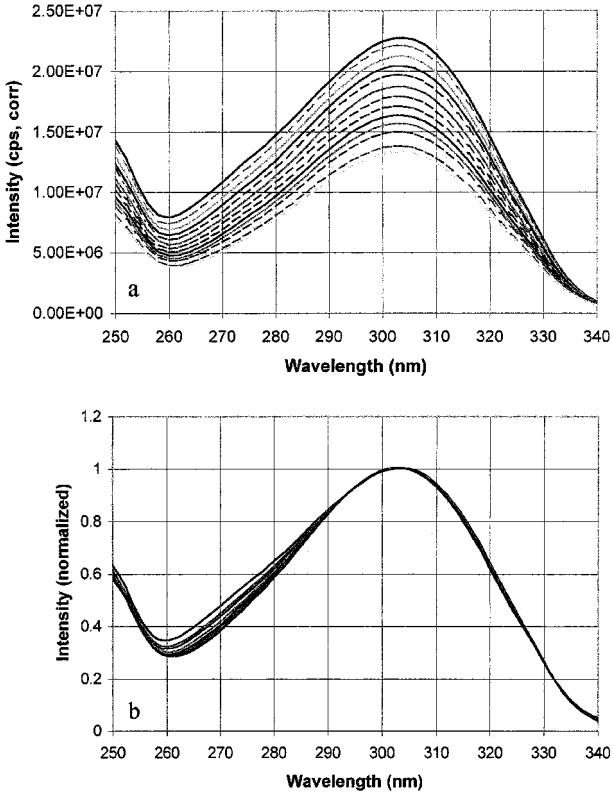

Fig. 3. Fluorescence excitation spectra of TT(2AP)TT pentanucleotide vs. temperature; temperatures approx every 5°C, from 7° to 65°C. (a) Raw spectra, corrected for lamp variations. (b) Normalized spectra. For clarity, some spectra from part a are not included.

RESULTS

Absorption spectra of the TT(2AP)TT/AATAA sample at 2 and 25°C, typical of 2AP-containing DNA, are shown in Fig. 2. The difference spectrum in part b of that figure shows that a slight shoulder develops in the normal-base region of this pentamer as temperature rises. The spectra of the other oligomers are similar, except that the relative amplitudes at 310 and 260 nm depend on the ratio of 2AP to normal bases (1:9 in the pentamer, 1:1 in (2AP)T). In a sample consisting of the pure free 2AP base, the second excited state of 2AP absorbs near 250 nm, with a minimum near 260–265 nm. The absorbance of normal bases in oligonucleotide samples is seen in the 260–280-nm region. Except for A(2AP)T and TT(2AP)TT/AATAA, the absorbance of samples at 260 nm and 320 nm changes by less than 1% from 2 to 45°C, indicating little hypochromic interaction between 2AP and its neighbor(s) in this temperature range. The duplex pentamer absorbance at 260 nm increases almost linearly by 6% from 2 to 45°C. As the fluorescence data will show, the "duplex" is probably duplex, as shown by the different temperature dependencies of the excitation spectral shifts of the double- and single-stranded pentamers.

Normalized fluorescence excitation spectra, used to illustrate spectral shifts of 2AP, are similar to the absorption spectrum of the 2AP free base (Fig. 3). The 260- to 280-nm excitation peak of the normal bases is largely absent, since the fluorescence quantum yields of normal bases are all less than 0.1%. The A(2AP)T sample, however, shows a small rise in intensity near 270 nm. We have shown that this is due to energy transfer from A to 2AP, which can approach 100% under optimal conditions [31,32,47]. Other bases adjacent to 2AP do transfer, but the efficiency is an order of magnitude less.

Artificial difference spectra of the free base (Fig. 4a), calculated by shifting the measured spectrum by a few nm and subtracting from the original, illustrate the characteristic antisymmetry (negative/positive bands)

[4] For serious quantitation of spectra changing in a complex manner, methods such as singular-value decomposition (SVD), other matrix methods, or global fitting should be explored [50–52]. (The difference method is, in fact, almost the same as the first step used in SVD.)

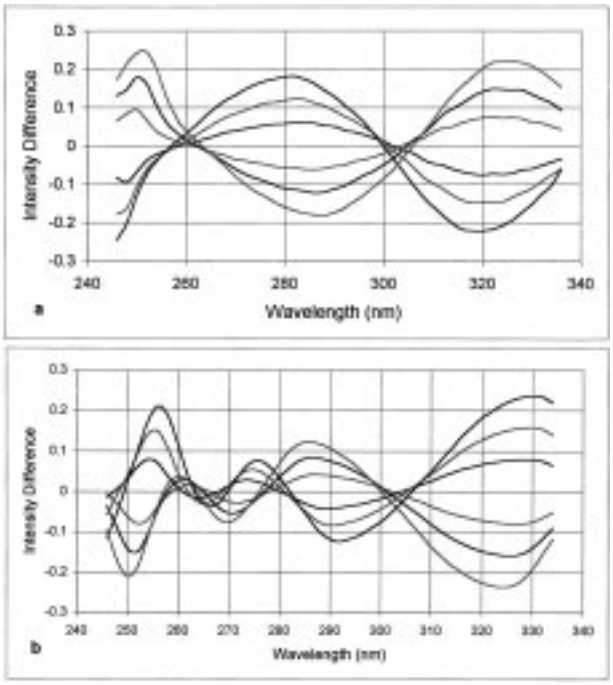

Fig. 4. (a) Difference spectra resulting from 2-nm incremental shifts of the fluorescence excitation spectrum of 2AP free base. Nearly antisymmetric spectra result, similar to those in Fig. 1a. The second excited state of 2AP can be seen near 250 nm. (b) Difference spectra of A(2AP)T oligomer. In addition to the higher excited state of 2AP, the A→2AP energy transfer band from 260–270 nm can be seen.

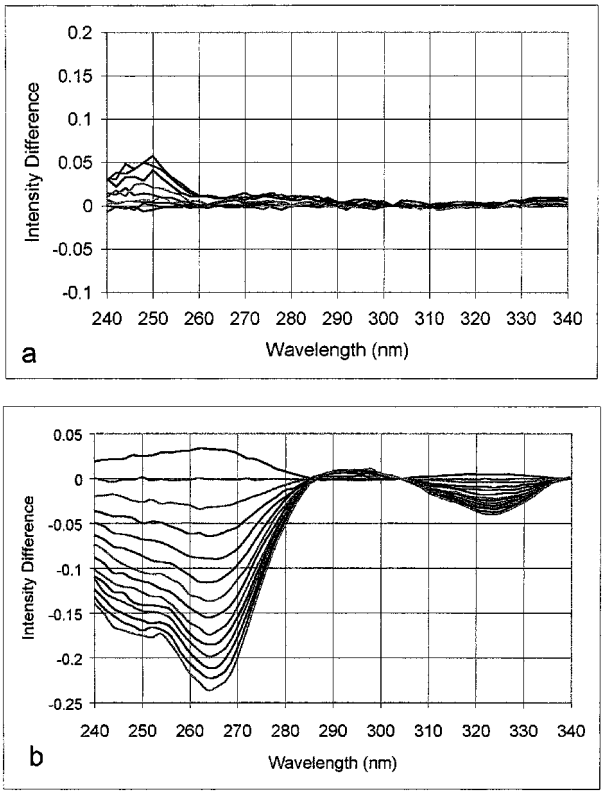

Fig. 5. Real difference spectra resulting from variation of temperature, 5–65°C. Higher temperatures correspond to more negative difference peaks at 265 and 323 nm. (a) 2AP free base. (b) A(2AP)T trinucleotide.

expected in difference spectra.[5] (2AP)T, G(2AP)C and C(2AP)G artificially-shifted spectra are similar to those of the free base. A(2AP)T, on the other hand, clearly shows the additional energy-transfer band in the 265-280-nm region (Fig. 4b).

Real difference spectra found from the temperature-dependent spectra are shown in Fig. 5 for the free base and A(2AP)T. While general features are the same as in Fig. 4, the oligonucleotide sample shows differences near the energy-transfer band, due to the strong temperature dependence of the transfer efficiency. As we have discussed this in detail elsewhere [47], we will focus attention on the difference band near 325 nm, where we do not have to worry about overlapping of two bands with two different temperature dependencies.

Figure 6 shows fluorescence excitation peak positions found from the parabolic fits to temperature-dependent spectra, fitting only the region near the peak. Two distinct features are evident. First, the excitation peaks for the G(2AP)C and C(2AP)G spectra are shifted far to

[5] These artificially shifted spectra are equivalent to the first derivative spectrum.

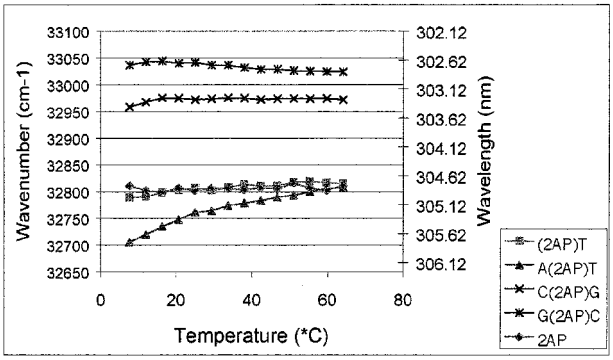

Fig. 6. Shifts of the peak of the fluorescence excitation spectra of 2AP free base and four ss oligomers, quantitated by the peak-fit method.

the blue of the other peaks. We have previously noted this blue shift for neighboring-G oligomers [31]. Second, the A(2AP)T sample shows far greater temperature dependence than the other ss oligomers. Looking more closely, the free base peak, found by the peak-fit method, is virtually temperature independent, as the C(2AP)G peak also appears to be. The G(2AP)C peak apparently

shifts slightly to the red with increasing temperature, in contrast to (2AP)T and A(2AP)T, which shift to the blue. The spectral difference method, which eliminates the absolute differences in peak position between the various samples, as well as quantitates the spectral shifts differently, shows the temperature dependences more clearly (Fig. 7). Three categories of peak wavelength vs. temperature dependence can be seen: (i) approximate temperature independence for 2AP free base, (ii) large negative slope for A(2AP)T, (iii) small negative slope for (2AP)T, C(2AP)G and G(2AP)C (assuming approximately linear dependence on temperature; see also TT(2AP)TT data; Fig. 10). A replotting of Fig. 7 as $N_aE_{ph} = N_ahc/\lambda$ vs 1/2 RT, where N_a = Avogadro's number, E_{ph} = energy of a photon at the peak of the excitation spectrum (as calculated from the difference method, the slope of which represents the change in electronic excitation energy of the incorporated 2AP per unit of thermal energy added per degree of freedom, yields values shown in Table I. As implied in the table, the linearity of the plots varies from sample to sample. These numbers should be considered, at present, to be phenomenological, but they have the advantage of being dimensionless.

All samples studied decrease in fluorescence yield as temperature increases (Fig. 8). Perhaps surprisingly, the 2AP free base decreases in yield most rapidly; the A(2AP)T oligo least rapidly.

The effect of double-helix formation on the spectral shift is shown in Figs. 9 and 10. As the predicted melting temperature of the oligomer is low,[6] differences are expected only in the low temperature region. We therefore focus in this region, where the temperature dependence is stronger. In Fig. 10b, the curve for the ds has been displaced upward for clarity and to emphasize that in the ds→ ss transition, the spectra at high temperature should be close to identical. (Recall that in the difference method the zero of spectral shift is, by definition, at the temperature of the reference spectrum, which has been chosen in this study to be the average of the three lowest temperature spectra).

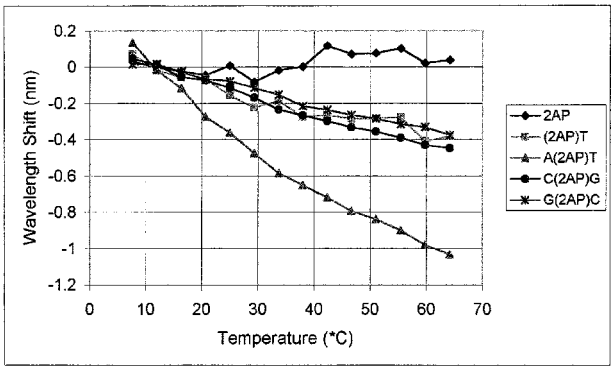

Fig. 7. Shifts of the peak of the fluorescence excitation spectra of 2AP free base and four ss oligomers, quantitated by the difference method.

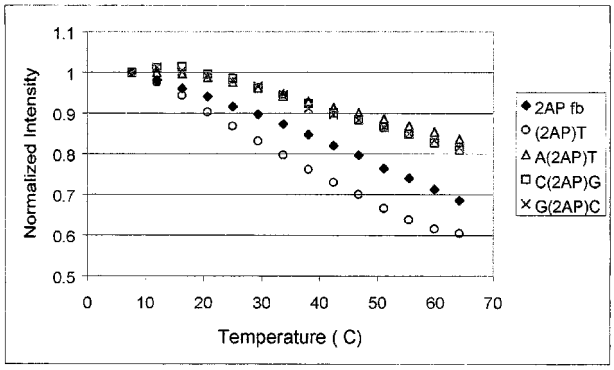

Fig. 8. Temperature dependence of the fluorescence intensity as a function of temperature for 2Ap and 4 ss oligomers. The absolute fluorescence amplitudes cannot be directly compared because of differing concentrations.

DISCUSSION

The primary objective of this work was to demonstrate simple and reliable spectroscopic methods for char-

Table I. Temperature Dependence of Excitation Spectra

Oligonucleotide	$\Delta E_e/\Delta E_{th}$[a]	Temperature dependence of intensity (°C^{-1})[b]
2AP free base	~0	0.0058
(2AP)T	0.39/0.80	0.0073
G(2AP)C	0.48/0.57	0.0041
C(2AP)G	0.54/0.81	0.0043
A(2AP)T	1.1/2.3	0.0034
TT(2AP)TT	0.35/0.90	0.0076
TT(2AP)TT/AATAA	0.43/1.8	0.0077

[a] Excitation spectrum energy shift per unit thermal energy change: high-temperature/low-temperature region. Given by local slopes in Figs. 7 and 10. A larger difference between high- and low-temperature values reflects greater nonlinearity of the graph. Absolute errors approx. ±0.1.

[b] Slope of intensity vs. temperature plot (as in Fig. 8; high temperature region, 20–65°C), normalized at low temperature. Absolute errors approx. ±0.02.

[6] T_m found from the program of Le Novere [53], using a variety of standard nearest-neighbor parameters and salt correction factors, ranged from +8 to −101°C for the TTATT/AATAA oligomer at our concentration. In retrospect, TT(2AP)TT seems a poor choice for the ss/ds comparison, but we find similar results for higher-melting-temperature oligomers (2AP)AAAA/TTTTT and A(2AP)AAA/TTTTT at higher concentrations (paper in preparation).

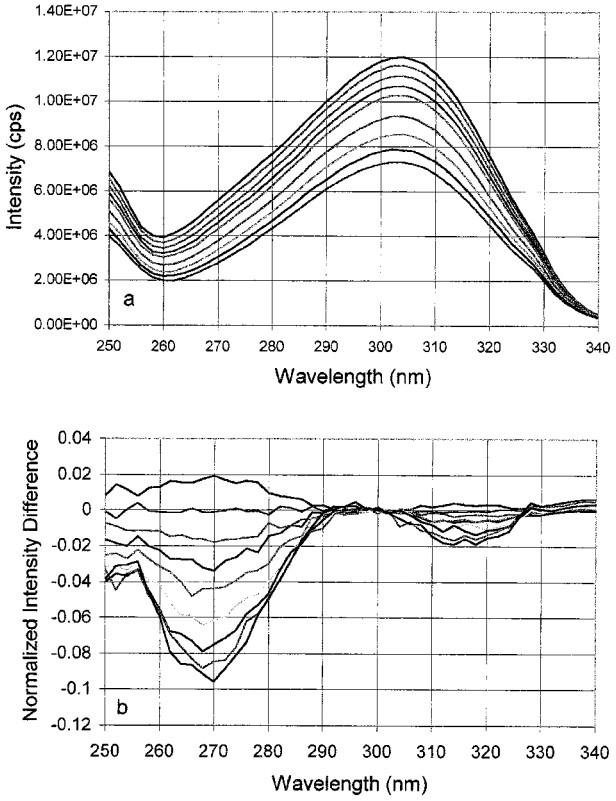

Fig. 9. (a) Fluorescence excitation spectra (not normalized) and (b) difference spectra vs temperature for TT(2AP)TT/AATAA. Temperatures range from 7°C (uppermost curve in a), to 64°C (lowermost curve in a). The largest-amplitude difference spectrum in b is at 64°C, both at 270 and 316 nm. The reference spectrum which was subtracted from each spectrum was obtained as the average of the 7°, 12° and 16°C spectra, resulting in the crossing of the two curves in b near 12°C. The energy-transfer band is clearly evident near 270 nm in part b.

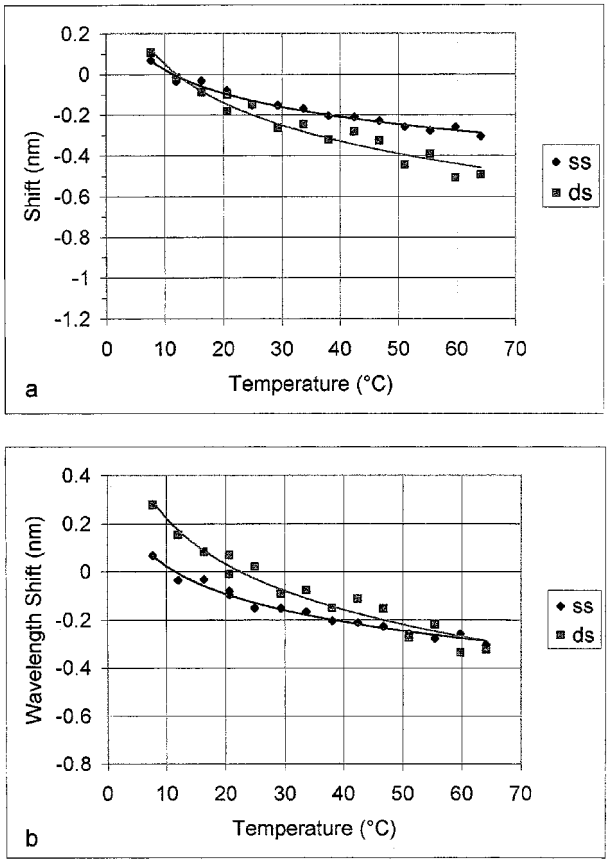

Fig. 10. Fluorescence spectral shifts of the TT(2AP)TT/AATAA and TT(2AP)TT oligomers as a function of temperature, determined from the difference method (315–320) nm in Fig. 9). (a) Shift calculated as in Fig. 9 (reference spectrum chosen as average of lowest three temperatures). (b) Double stranded shift moved upwards to emphasize low temperature dependence. See text. The shifts are comparable to those of (2AP)T, C(2AP)G and G(2AP)C ss oligos in Fig. 7, but less than those of the A-containing oligo. The duplex shifts further and shows more curvature, especially from 5–15°C.

acterizing steady-state fluorescence of the modified DNA base, 2-aminopurine, depending upon the surrounding bases and temperature. The samples studied were single-stranded, short oligonucleotides and one single- and double-stranded pentanucleotide. The results show that the temperature dependence of the excitation spectrum, though small, is easily measured and quantified using an Excel spreadsheet.

For the ss oligomers measured, Figs. 7 and 10 show three categories of temperature dependence: almost none for the 2AP free base; moderate for (2AP)T, C(2AP)G, G(2AP)C and TT(2AP)TT, and strong for A(2AP)T. The spectral shifts clearly depend upon the neighbors of 2AP, with the stronger stacking tendency of A with 2AP likely responsible for the stronger temperature dependence. The blue-shifted excitation spectra of G(2AP)C (esp) and C(2AP)G, clearly identify these neighbors, but the bluer spectra are not accompanied by a stronger temperature dependence. Adenine neighboring 2AP can be detected both through the stronger spectral shift temperature dependence, as well as through the temperature-dependent energy-transfer band in the 260–270-nm excitation region. In difference spectra, this transfer band can be observed breaking the approximate antisymmetry of the temperature-dependent difference spectra (Fig. 4b). We have thoroughly discussed this elsewhere [47,54].

Formation of a duplex causes somewhat greater temperature dependence of the excitation spectra. However, the differences between TT(2AP)TT and TT(2APTT/AATAA are not large. Double-strand formation is expected only at the lowest temperatures; the temperature dependence for the ds pentamer is indeed greater than that of the ss between 5 and 15°C, but the differences

are small when compared to A(2AP)T. We have observed that ds→ss changes are small compared to stacking changes also in higher-melting temperature (2AP)AAAA/TTTTT and A(2AP)AAA/TTTTT oligomers. We will present these results elsewhere.

Two spectral analysis methods have been employed in the present study. Both emphasize simplicity and robustness, not sophistication. Of the two methods, the spectral difference method is more robust in that it has less dependence on the individual's choice of analytic parameters. It has, in fact, no parameters to choose, whereas the peak-fitting method suffers from dependence on the fraction of each spectrum fit. The difference method also allows easy identification of more complex spectral perturbations in the difference spectra; the fitting method does not. While more sophisticated fitting methods (e.g., singular-value decomposition) can also characterize complex spectral changes, this analytic tool is not as widely available as an Excel spreadsheet and is more difficult to implement. It is also noteworthy that 0.1-nm spectral shifts are quantitated with good precision even though fluorescence data was recorded only every 2 nm. In fact, the precision of the shift is governed mostly by the spectral signal-to-noise ratio, as with any difference method. While the present work focuses on giving a useful analytic tool to the DNA biophysicist/biochemist/molecular biologist, a detailed spectroscopic understanding of the shifting bands is nevertheless needed in the future. One notes, for example, in the details of the duplex difference spectra (Fig. 9b; long-wavelength region), the spectral changes are more complex than spectral shifts. We will address this in future work.

Table I shows a summary of the temperature dependencies of spectral properties we have measured. The temperature dependence of the excitation spectral shift, measured by the dimensionless electronic-energy increase per unit thermal energy increase, $\Delta E_e/\Delta E_{th}$, is shown in the first column in the table, with values calculated from high- and low-temperature regions of the graphs in Figs. 7 and 10. Differences between the two values indicate degree of departure from linearity, e.g., G(2AP)C and C(2AP)G are close to linear, while A(2AP)T, TT(2AP)TT and TT(2AP)TT/AATAA are not. Higher values indicate more rapid spectral shift vs. temperature. The free base has practically no spectral shift with temperature. A single neighboring adenine results in 2–3 times the spectral temperature sensitivity as an oligonucleotide with other neighboring bases. The temperature dependence of the fluorescence intensity does not parallel that of the spectral shift. Since fluorescence yield depends upon quenching mechanisms, and not perturbations of the excited-state spectra, this differing dependence is not completely unexpected. It is nevertheless surprising that the strongest spectral-shift dependence for ss DNA, observed for A(2AP)T, is associated with the weakest yield dependence on T. The relatively small spectral shift dependence of G(2AP)C is also associated with the largest intensity dependence. Clearly the G base interacts with 2AP, but in a way which makes fluorescence yield more temperature sensitive, but not the excitation energy. Stacking of A may again clarify the differential sensitivity of oligomers to temperature, since higher temperature reduces stacking, tending to increase fluorescence, but at the same time, higher temperature reduces the intrinsic yield (increases quenching) of 2AP, as seen in the free base. The effects thus tend to offset one another.

The present work does not address the important question of the length dependence of spectral changes of incorporated 2-aminopurine in DNA. Work in progress will show how the 2AP excitation spectrum behaves in much longer DNA, which may locally unstack or unwind in response to temperature or protein binding.

ACKNOWLEDGMENTS

This work was supported in part by grants from the National Science Foundation MCB-9723278 and Research Experiences for Undergraduates grant DMR 9619405 (support of M. J. Lee).

REFERENCES

1. N. Hagag, E. R. Birnbaum, and D. W. Darnall (1983) *Biochemistry* **22**, 2420–2427.
2. J. R. Lakowicz, I. Gryczynski, W. Wiczk, G. Laczko, F. C. Prendergast, and M. L. Johnson (1990) *Biophys. Chem.* **36**, 99–115.
3. P. Wu and L. Brand (1994) *Anal. Biochem.* **218**, 1–13.
4. P. R. Selvin (1995) *Methods Enzymol.* **246**, 300–334.
5. M. P. Lillo, B. K. Szpikowska, M. T. Mas, J. D. Sutin, and J. M. Beechem (1997) *Biochemistry* **36**(37), 11273–11281.
6. W. J. Dong, J. Xing, M. Villain, M. Hellinger, J. M. Robinson, M. Chandra, R. J. Solaro, P. K. Umeda, and H. C. Cheung (1999) *J. Biol. Chem.* **274**(44), 31382–31390.
7. O. Tcherkasskaya and O. B. Ptitsyn (1999) *Protein Eng.* **12**(6), 485–490.
8. M. Li, L. G. Reddy, R. Bennett, N. D. Silva, Jr., L. R. Jones, and D. D. Thomas (1999) *Biophys. J.* **76**(5), 2587–2599.
9. W. J. Dong, J. M. Robinson, J. Xing, P. K. Umeda, and H. C. Cheung (2000) *Protein Sci.* **9**(2), 280–289.
10. R. A. Keller, L. A. Bottomly, and N. J. Dovichi (eds.) (1992) in R. A. Keller, L. A. Bottomly, and N. J. Divichi (Eds.), *Advances in DNA Sequencing Technology,* SPIE, Los Angeles, Vol. 1891.
11. S. C. Hung, R. A. Mathies, and A. N. Glazer (1998) *Anal. Biochem.* **255**(1), 32–38.
12. A. Van Orden, H. Cai, P. M. Goodwin, and R. A. Keller (1999) *Anal. Chem.* **71**(11), 2108–2116.

13. M. Sauer, B. Angerer, K. T. Han, and C. Zander (1999) *Phys. Chem. Chem. Phys.* **1**(10), 2471–2477.
14. S. McWhorter and S. A. Soper (2000) *Electrophoresis* **21**(7), 1267–1280.
15. A. Ujvari and C. T. Martin (1996) *Biochemistry* **35**(46), 14574–14582.
16. Y. Jia, A. Kumar, and S. S. Patel (1996) *J. Biol. Chem.* **271**(48), 30451–30458.
17. B. W. Allan, N. O. Reich, and J. M. Beechem (1999) *Biochemistry* **38**(17), 5308–5314.
18. L. B. Bloom, M. R. Otto, J. M. Beechem, and M. F. Goodman (1993) *Biochemistry* **32**, 11247–11258.
19. L. B. Bloom, M. R. Otto, R. Eritja, L. J. Reha-Krantz, M. F. Goodman, and J. M. Beechem (1994) *Biochemistry* **33**, 7576–7586.
20. K. D. Raney, L. C. Sowers, D. P. Millar, and S. J. Benkovic (1994) *Proc. Natl. Acad. Sci. USA* **91**, 6644–6648.
21. B. W. Allan and N. O. Reich (1996) *Biochemistry* **35**(47), 14757–14762.
22. J. M. Beechem, M. R. Otto, L. B. Bloom, R. Eritja, L. J. Reha-Krantz, and M. F. Goodman (1998) *Biochemistry* **37**(28), 10144–10155.
23. M. R. Otto, L. B. Bloom, M. F. Goodman, and J. M. Beechem (1998) *Biochemistry* **37**(28), 10156–10163.
24. L. J. Reha-Krantz, L. A. Marquez, E. Elisseeva, R. P. Baker, L. B. Bloom, H. B. Dunford, and M. F. Goodman (1998) *J. Biol. Chem.* **273**(36), 22969–22976.
25. W. C. Lam, E. J. Van der Schans, L. C. Sowers, and D. P. Millar (1999) *Biochemistry* **38**(9), 2661–2668.
26. M. Aida, K. Yamane, and C. Nagata (1986) *Mutat. Res.* **173**(1), 49–54.
27. W. P. Diver and D. M. Woodcock (1989) *Mutagenesis* **4**(4), 302–305.
28. G. Speit, S. Garkov, S. Haupter, and B. Koberle (1990) *Mutagenesis* **5**(2), 185–190.
29. L. A. Marquez and L. J. Rehakrantz (1996) *J. Biol. Chem.* **271**(46), 28903–28910.
30. M. F. Goodman and K. D. Fygenson (1998) *Genetics* **148**(4), 1475–1482.
31. D. Xu (1996) University of Alabama at Birmingham.
32. T. M. Nordlund, D. Xu, and K. O. Evans (1993) *Biochemistry* **32**, 12090–12095.
33. T. M. Nordlund, D. Xu, and K. Evans (1994) *Proc. SPIE* **2137**, 634–643.
34. S. O. Kelley and J. K. Barton (1999) *Science* **283**(5400), 375–381.
35. P. O. Lycksell, A. Gräslund, F. Claesens, L. W. McLaughlin, U. Larsson, and R. Rigler (1987) *Nucleic Acids Res.* **15**(21), 9011–9025.
36. A. Gräslund, F. Claesens, L. W. McLaughlin, P.-O. Lycksell, U. Larsson, and R. Rigler (1987) in A. Ehrenberg, R. Rigler, A. Gräslund, and L. Nilsson (Eds.), *Structure, Dynamics and Function of Biomolecules*, Springer-Verlag, Berlin, pp. 201–207.
37. T. M. Nordlund, S. Andersson, L. Nilsson, R. Rigler, A. Gräslund, and L. W. McLaughlin (1989) *Biochemistry* **28**(23), 9095–9103.
38. P. G. Wu, T. M. Nordlund, B. Gildea, and L. W. McLaughlin (1990) *Biochemistry* **29**(27), 6508–14.
39. K. Evans, D.-G. Xu, Y.-S. Kim, and T. M. Nordlund (1992) *J. Fluoresc.* **2**(4), 209–216.
40. D. Xu, K. O. Evans, and T. M. Nordlund (1994) *Biochemistry* **33**, 9592–9599.
41. D. P. Millar and T. E. Carver (1994) *Proc. SPIE* **2137**, 686–695.
42. D. P. Millar (1996) *Curr. Opin. Struct. Biol.* **6**(3), 322–326.
43. D. C. Ward, E. Reich, and L. Stryer (1969) *J. Biol. Chem.* **244**, 1228–1237.
44. A. Kawski, B. Bartoszewicz, I. Gryczynski, and M. Krajewski (1975) *Bull. Acad. Polonaise Sci.* (*Ser. Sci. Math. Astr. Phys.*) **XXIII**, 367–372.
45. A. Bierzynski, H. Kozlowska, and K. L. Wierzchowski (1977) *Biophys. Chem.* **6**, 223–229.
46. J. D. Puglisi and I. J. Tinoco (1989) in J. E. Dahlberg and J. N. Abelson (Eds.), *RNA Processing Part A. General Methods*, Academic Press, San Diego, Vol. 180, pp. 304–325.
47. D. Xu and T. M. Nordlund (2000) *Biophys. J.* **78**(2), 1042–1058.
48. W. Knox, T. M. Nordlund, and G. Mourou (1982) *Appl. Phys. B* **28**, 174–175.
49. D. Xu, K. O. Evans, and T. M. Nordlund (1994) *Biochemistry* **33**(32), 9592–9599.
50. J. Beechem and L. Brand (1985) *Ann. Rev. Biochem.* **54**, 43–71.
51. J. H. Sommer, T. M. Nordlund, M. McGuire, and G. McLendon (1986) *J. Phys. Chem.* **90**, 5173–5178.
52. E. R. Henry (1997) *Biophys. J.* **72**(2), 652–673.
53. N. Le Novere (2000) http://bioweb.pasteur.fr/seqanal/interfaces/melting.html.
54. T. M. Nordlund, D. Xu, and K. O. Evans (1993) *Biochemistry* **32**(45), 12090–12095.